Wind and Structures, Vol. 1, No. 3 (1998) 243-253
DOI: http://dx.doi.org/10.12989/was.1998.1.3.243

Numerical analysis of interference galloping of two identical circular cylinders

E. Bł azik-Borowa† and A. Flaga‡

Department of Structural Mechanics, Faculty Civil and Sanitary Engineering, Lublin Technical University, ul. Nadbystrzycka 40, 20-618 Lublin, Poland

Abstract. The paper deals with numerical analysis of interference galloping of two elastically supported circular cylinders of equal diameters. The basis of the analysis is quasi-steady model of this phenomenon. The model assumes that both cylinders participate in process of interference galloping and they have two degrees of freedom. The movement of the cylinders is written as a set of four nonlinear differential equations. On the basis of numerical solutions of this equations the authors evaluate the correctness of this quasi-steady model. Then they estimate the dependence of a critical reduced velocity on the Scruton number, turbulence intensity and arrangements of the cylinders.

Key words: aerodynamic interference; a cylinder; interference galloping; the quasi-steady theory; the numerical analysis.

1. Introduction

Interference galloping is one of bistable flows being aerodynamic phenomena. It exists during the aerodynamic interference of two circular cylinders. There are some critical regions of the position of the downstream cylinder in which vibrations of both cylinders caused by interference galloping may occur. One of them satisfies the following conditions for a staggered arrangement : $L_x/D \in (1.5\,;3.5)$ and $\beta \in (5^\circ\,;15^\circ)$, where : L_x - distance between the midpoints of the cylinders ; D - cylinder diameter ; β - angle between the average wind direction and the axis joining the midpoints of the cylinders. This phenomenon was subject to many experiments in wind tunnels and a few measurements in natural scale. The measurement results and exact description of interference galloping can be found in such articles as : Zdravkovich and Pridden (1977), Ruscheweyh (1983), Ruscheweyh and Dielen (1992), Kazakiewicz, Grafskij, Riedko (1985), Shiraishi, Matsumoto, Shirato (1986), Matsumoto, Shiraishi, Shirato (1990), Sun and Gu (1995), Bł azik-Borowa, Flaga, Kazakiewicz (1996), Watzinger (1996).

Nowadays several mathematical models of interference galloping are known, too (comp. Kazakiewicz, Grafskij, Riedko 1985, Matsumoto, Shiraishi, Shirato 1990, Ruscheweyh and Dielen 1992, Dielen and Ruscheweyh 1995). One of them is a quasi-steady model of interference galloping, which has been elaborated by the authors and it has been described in detail in Bł azik-Borowa and Flaga (1996), Bł azik-Borowa and Flaga (1995).

† Doctor
‡ Professor

The phenomenon of interference galloping is also described with the FEM method (comp. Sockel and Watzinger 1997).

2. The principal assumptions and relations

The following simplifying assumptions have been accepted during the construction of a quasi-steady model of interference galloping :

- diameters of crosswise intersections of cylinders are equal ;
- position of a downstream cylinder is found within the region with the following limitations : $2 < L_x/D < 4$; $5° < \beta < 15°$, that is : in the region of bistable flows (comp. Fig. 1) ;
- cylinders are made of rigid material ;
- flow is viscous and incompressible ;
- cylinders are elastically supported and they have two degrees of freedom : along the average wind direction and in the direction perpendicular to it ;
- boundary disturbance effects are neglected;
- problem is treated as flat;
- global coordinate system is linked to the midpoint of an upstream cylinder and x axis is parallel to the average wind direction ;
- quantities such as : the instantaneous wind velocity V_s, the components of the instantaneous wind velocity towards x and y axes u_s and v_s, the instantaneous angle of wind attack γ_s, are the average values from the region of averaging $S = \Delta y x H$, where : $H = \kappa_1 D$; $\Delta y = \kappa_2 D$ - the across dimension of the wake formed behind the two cylinders κ_1, $\kappa_2 \in (5 \div 10)$. The spatial region of averaging is located in front of an upstream cylinder in the distance at least D (comp. Fig. 1) ;
- aerodynamic load is constant on entire length of cylinders;
- determination of the physical model and then the mathematical one of a wind load for upstream and downstream cylinders is based on a dimensional analysis and quasi-steady

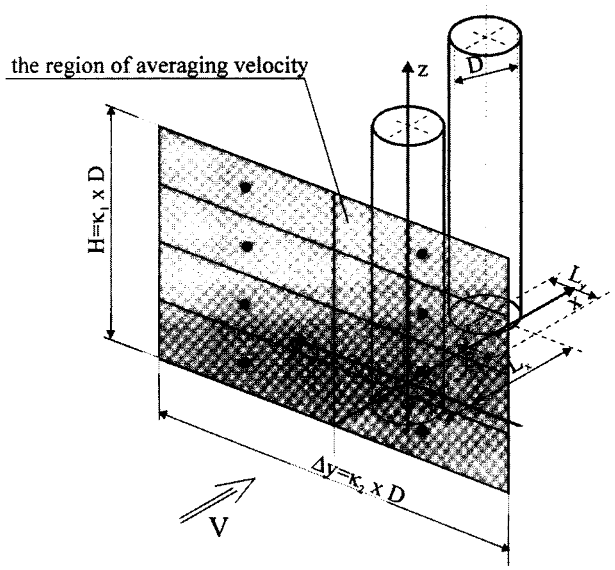

Fig. 1 Arrangement of points in which flow field is generated

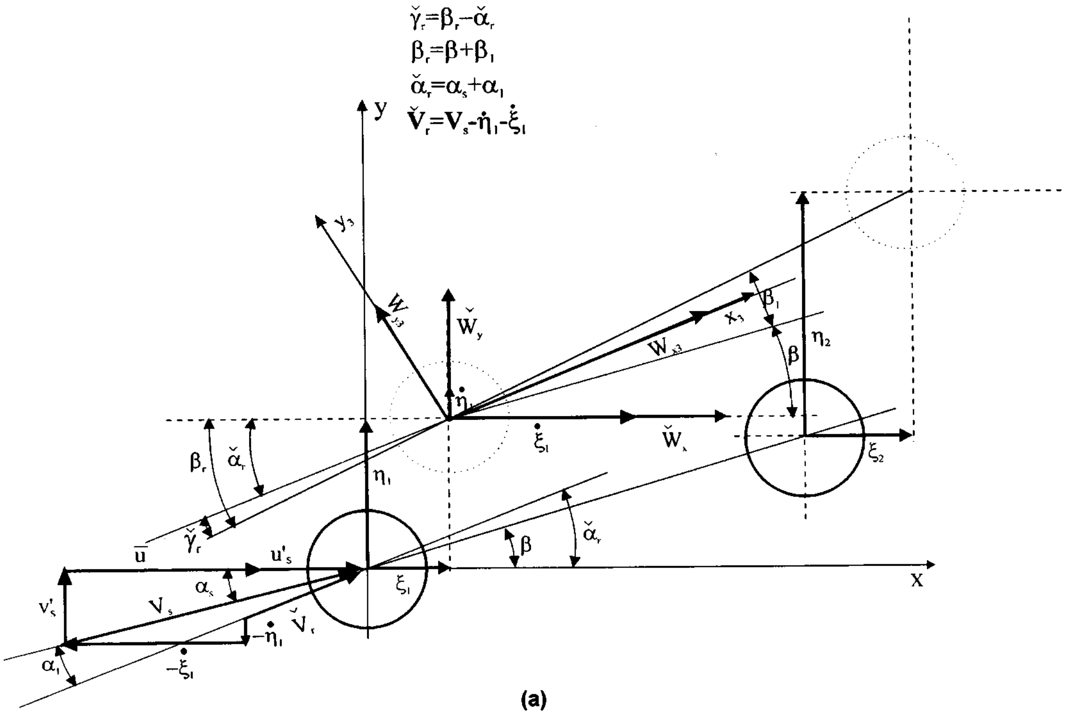

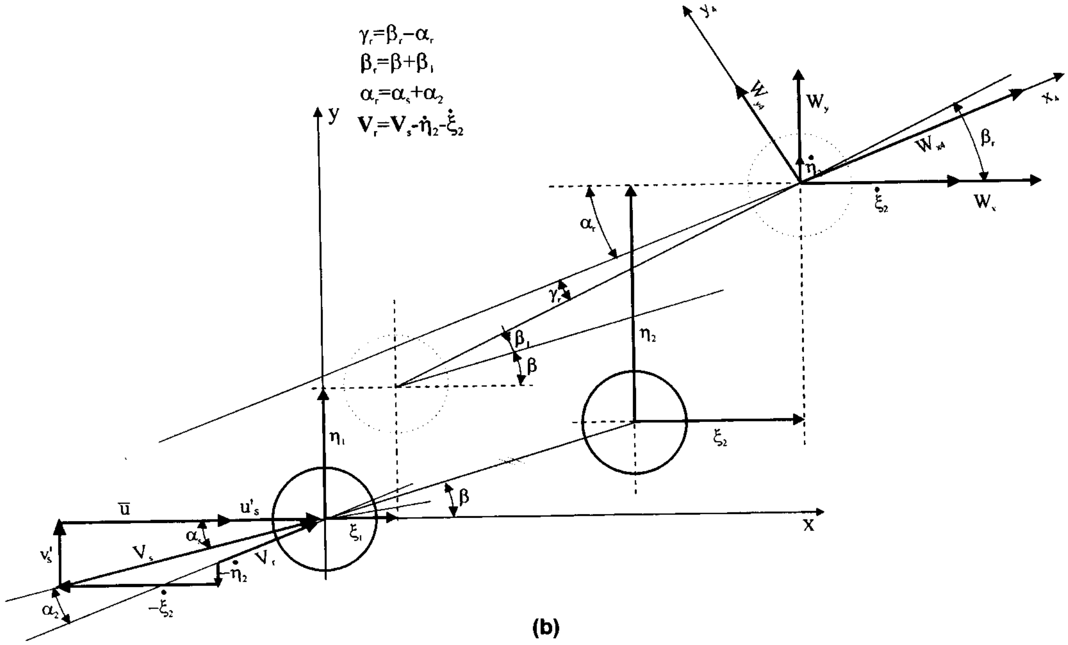

Fig. 2 The cylinders arrangement, the components of wind and the other important symbols; a) for the upstream cylinder; b) for the downstream cylinder

theory in aerodynamics of slender structures.

Assuming appropriate trigonometric dependence (comp. Fig. 2), the components of wind load towards the axis of a global coordinate system influencing the upstream cylinder $\breve{W}_x$, $\breve{W}_y$ and downstream cylinder W_x, W_y can be given by :

- for the upstream cylinder

$$\breve{W}_x(\breve{\alpha}_r, \breve{\gamma}_r) = [\breve{W}_{x3}(\breve{\gamma}_r)\cos\breve{\alpha}_r - \breve{W}_{y3}(\breve{\gamma}_r)\sin\breve{\alpha}_r] \tag{1}$$

$$\breve{W}_y(\breve{\alpha}_r, \breve{\gamma}_r) = [\breve{W}_{x3}(\breve{\gamma}_r)\sin\breve{\alpha}_r + \breve{W}_{y3}(\breve{\gamma}_r)\cos\breve{\alpha}_r] \tag{2}$$

- for the downstream cylinder

$$W_x(\alpha_r, \gamma_r) = [W_{x4}(\gamma_r)\cos\alpha_r - W_{y4}(\gamma_r)\sin\alpha_r] \tag{3}$$

$$W_y(\alpha_r, \gamma_r) = [W_{x4}(\gamma_r)\sin\alpha_r + W_{y4}(\gamma_r)\cos\alpha_r] \tag{4}$$

where : $\breve{W}_{x3}$, $\breve{W}_{y3}$ - components of interferential load on the length unit of the upstream cylinder along axes x_3 and y_3, respectively; W_{x4}, W_{y4} - components of interferential load on the length unit of the downstream cylinder along axes x_4 and y_4, respectively. The axes x_3 and y_3 are directed along and across the direction of the relative velocity $\breve{V}_r$ of the upstream cylinder, and the axes x_4 and y_4 are directed along and across the direction of the relative velocity V_r of the downstream one (Fig. 2).

On the basis of dimensional analysis, the above components of aerodynamic load can be written as follows :

$$\breve{W}_i(\breve{\gamma}_r) = \frac{1}{2}\rho\breve{V}_r D\breve{C}_i(\breve{\gamma}_r), \; i = x_3, y_3 \tag{5}$$

$$W_i(\gamma_r) = \frac{1}{2}\rho V_r D C_i(\gamma_r), \; i = x_4, y_4 \tag{6}$$

where : ρ - air mass density; $\breve{C}_{x3}(\breve{\gamma}_r) = \breve{C}_{x3}^{st}(\breve{\gamma}_r) = \breve{C}_x(\beta = \breve{\gamma}_r)$, $\breve{C}_{y3}(\breve{\gamma}_r) = \breve{C}_{y3}^{st}(\breve{\gamma}_r) = \breve{C}_y(\beta = \breve{\gamma}_r)$, $C_{x4}(\gamma_r) = C_{x4}^{st}(\gamma_r) = C_x(\beta = \gamma_r)$, $C_{y4}(\gamma_r) = C_{y4}^{st}(\gamma_r) = C_y(\beta = \gamma_r)$ - static aerodynamic drag coefficient and lift coefficient for the upstream and the downstream cylinders respectively. These aerodynamic coefficients of both cylinders are obtained for a particular case that is when the cylinders do not vibrate so they do not change their location and at the same the wind velocity and direction are constant. It means that the angle of wind attack $\beta = \breve{\gamma}_r$ or $\beta = \gamma_r$ respectively.

The relative angles of wind attack are angles between the direction of a respective relative velocity and a line joining centers of displaced cylinders (cylinders in new location) and they are described by the equations (Fig. 2) :

- for the upstream cylinders

$$\breve{\gamma} = \breve{\gamma}(z, t) = (\beta + \beta_1) - (\alpha_s + \alpha_1) = \beta_r - \breve{\alpha}_r \tag{8}$$

$$\breve{\gamma}_r = \arctan\frac{L_x\tan\beta u_s - L_x\tan\beta\dot{\xi}_1 + \eta u_s - \eta\dot{\xi}_1 - v_s' L_x - v_s'\xi + \dot{\eta}_1 L_x + \dot{\eta}_1\xi}{L_x u_s - L_x\dot{\xi}_1 + \xi u_s - \xi\dot{\xi}_1 + L_x\tan\beta v_s' - L_x\tan\beta\dot{\eta}_1 + \eta v_s' - \eta\dot{\eta}_1} \tag{9}$$

- for the downstream cylinders

$$\gamma = \gamma(z, t) = (\beta + \beta_1) - (\alpha_s + \alpha_2) = \beta_r - \alpha_r \tag{10}$$

$$\gamma_r = \arctan \frac{L_x \tan \beta u_s - L_x \tan \beta \dot{\xi}_2 + \eta u_s - \eta \dot{\xi}_2 - v_s' L_x - v_s' \xi + \dot{\eta}_2 L_x + \dot{\eta}_2 \xi}{L_x u_s - L_x \dot{\xi}_2 + \xi u_s - \xi \dot{\xi}_2 + L_x \tan \beta v_s' - L_x \tan \beta \dot{\eta}_2 + \eta v_s' - \eta \dot{\eta}_2} \tag{11}$$

where : ξ_1, η_1, ξ_2, η_2 - components of displacement of the upstream and downstream cylinders towards the x and y axes, respectively; $\xi = \xi_2 - \xi_1$; $\eta = \eta_2 - \eta_1$.

Presuming that each cylinder is a system with two degrees of freedom, the equations describing the movement of these cylinders towards the axis x and y can be written in the following form :

- for the upstream cylinder

$$m\ddot{\xi}_1(t) + C_{\xi_1}\dot{\xi}_1(t) + K_{\xi_1}\xi_1(t) = \breve{W}_x(t) \tag{12}$$

$$m\ddot{\eta}_1(t) + C_{\eta_1}\dot{\eta}_1(t) + K_{\eta_1}\eta_1(t) = \breve{W}_y(t) \tag{13}$$

- for the downstream cylinder

$$m\ddot{\xi}_2(t) + C_{\xi_2}\dot{\xi}_2(t) + K_{\xi_2}\xi_2(t) = W_x(t) \tag{14}$$

$$m\ddot{\eta}_2(t) + C_{\eta_2}\dot{\eta}_2(t) + K_{\eta_2}\eta_2(t) = W_y(t) \tag{15}$$

where : m - mass per length unit of the cylinder; K_{ξ_1}, K_{η_1}, K_{ξ_2}, K_{η_2}, C_{ξ_1}, C_{η_1}, C_{ξ_2}, C_{η_2} - damping and stiffness coefficients of the upstream and downstream cylinder towards the axis x and y, respectively; $\dot{\xi}_1$, $\dot{\eta}_1$, $\dot{\xi}_2$, $\dot{\eta}_2$ - components of the velocity of the upstream and downstream cylinders towards the x and y axes, respectively; $\ddot{\xi}_1$, $\ddot{\eta}_1$, $\ddot{\xi}_2$, $\ddot{\eta}_2$ - components of the acceleration of the upstream and downstream cylinders towards the x and y axes, respectively.

On the basis of this model the authors obtained the following equation at first :

$$U_r^{cr} = \frac{2\,Sc}{\left.\dfrac{\partial C_y(\gamma_s)}{\partial \gamma_s}\right|_{\gamma_s = \beta} - C_x(\beta)} \tag{16}$$

where : U_r^{cr} - reduced critical velocity; Sc - Scruton number; $C_x(\beta)$, $\left.\dfrac{\partial C_y}{\partial \gamma_s}\right|_{\gamma_s = \beta}$ - static drag coefficient and derivative of static lift coefficient of downstream cylinder.

Eq. (16) can be used only for the small displacements of cylinders.

Secondly the movement of the cylinders towards the axes x (the average wind direction) and y (the direction perpendicular to the average wind direction) is expressed by a set of four nonlinear differential equations :

- for the upstream cylinder in the direction x

$$m\frac{2}{\rho D}\ddot{\xi}_1(t) + C_{\xi_1}\frac{2}{\rho D}\dot{\xi}_1(t) + K_{\xi_1}\frac{2}{\rho D}\xi_1(t) +$$
$$-(u_s \breve{C}_x(\breve{\gamma}_r) - v_s' \breve{C}_y(\breve{\gamma}_r) - \breve{C}_x(\breve{\gamma}_r)\dot{\xi}_1(t) + \breve{C}_y(\breve{\gamma}_r)\dot{\eta}_1(t))$$
$$\sqrt{(u_s - \dot{\xi}_1(t))^2 + (v_s' - \dot{\eta}_1(t))^2} = 0 \tag{17}$$

- for the upstream cylinder in the direction y

$$m\frac{2}{\rho D}\ddot{\eta}_1(t)+C_{\eta_1}\frac{2}{\rho D}\dot{\eta}_1(t)+K_{\eta_1}\frac{2}{\rho D}\eta_1(t)+$$
$$-(v_s'\breve{C}_x(\breve{\gamma}_r)+u_s\breve{C}_y(\breve{\gamma}_r)-\breve{C}_y(\breve{\gamma}_r)\dot{\xi}_1(t)-\breve{C}_x(\breve{\gamma}_r)\dot{\eta}_1(t))$$
$$\sqrt{(u_s-\dot{\xi}_1(t))^2+(v_s'-\dot{\eta}_1(t))^2}=0 \tag{18}$$

• for the downstream cylinder in the direction x

$$m\frac{2}{\rho D}\ddot{\xi}_2(t)+C_{\xi_2}\frac{2}{\rho D}\dot{\xi}_2(t)+K_{\xi_2}\frac{2}{\rho D}\xi_2(t)+$$
$$-(u_s C_x(\gamma_r)-v_s' C_y(\gamma_r)-C_x(\gamma_r)\dot{\xi}_2(t)+C_y(\gamma_r)\dot{\eta}_2(t))$$
$$\sqrt{(u_s-\dot{\xi}_2(t))^2+(v_s'-\dot{\eta}_2(t))^2}=0 \tag{19}$$

• for the downstream cylinder in the direction y

$$m\frac{2}{\rho D}\ddot{\eta}_2(t)+C_{\eta_2}\frac{2}{\rho D}\dot{\eta}_2(t)+K_{\eta_2}\frac{2}{\rho D}\eta_2(t)+$$
$$-(v_s' C_x(\gamma_r)+u_s C_y(\gamma_r)-C_y(\gamma_r)\dot{\xi}_2(t)-C_x(\gamma_r)\dot{\eta}_2(t))$$
$$\sqrt{(u_s-\dot{\xi}_2(t))^2+(v_s'-\dot{\eta}_2(t))^2}=0 \tag{20}$$

where : u_s and v_s' - spatially averaged components of wind velocity in the direction x and y.

3. Calculation methods

In the present paper interference galloping is analysed on the basis of the solution of the set of differential Eq. (17)~(20). It has been solved numerically with Runge-Kutty's method. The system of four differential equations of the second order has been replaced by the system of eight equations of the first order. The static aerodynamic coefficients as nonlinear functions of relative angle of wind attack were adopted, on the basis of experimental results available in publication Zdravkovich and Pridden (1977). This nonlinear functions have been replaced by broken lines.

A flow field is generated in eight points and it is represented by eight correlated random processes. Arrangement of points is shown in Fig. 1. The components of the wind velocity u_s and v_s are average velocities from eight random processes.

The calculations have been performed for cylinders modelling segments of ropes in a cable-stayed bridge in Prague. The measurement results of vibrations of stay-cables are presented by Studničkova (1994). The numerical analysis has been carried out for the following parameters :

• $D = 0.168$ m ;
• $m = 87.7$ kg/m ;
• $\omega_o = 6.41$ rad/s, where ω_o natural circular frequency of a cylinder ;
• $K_{\xi_1} = K_{\eta_1} = K_{\xi_2} = K_{\eta_2} = 3500$ N/m ;
• $\rho = 1.25$ kg/m^3.

Other parameters, such as : the logarithmic damping decrement, the distance between the

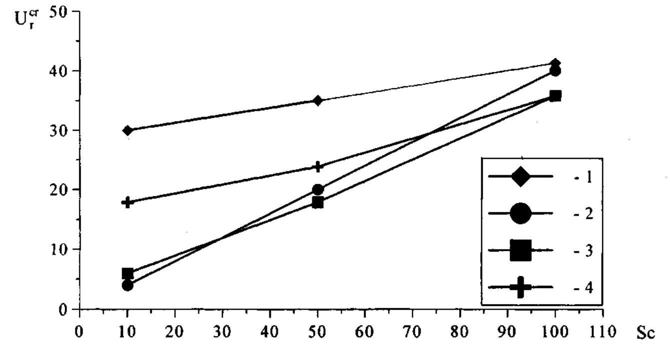

Fig. 3 The reduced critical velocity U_r^{cr} as function of Scruton number Sc for $L_x/D=2.1$ and $L_y/D=0.4$; 1 - experimental results obtained by Zdravkovich and Medeiros (1991) (turbulence intensity - $I_u=1\%$); 2 - calculated value on the basis of Eq. (16); 3 - numerical results at steady flow; 4 - numerical results at unsteady flow ($I_u=1\%$); where $I_u = \frac{\sigma}{\bar{u}_s} 100\,\%$

cylinders and the angle of wind attack, have been changed.

The experimental results and the first part of calculation results are shown in Fig. 3. The comparison is made to check quasi-steady model and method of calculation. All presented graphs of the reduced critical velocity are rising function of Scruton number. For Scruton number greater than about 50 it is the best conformity of all results. In Fig. 3 it is seen that if turbulence intensity is taken into consideration, then differences between the experimental and calculations results decrease.

4. Interference galloping at steady flow

This part of numerical analysis has been made at the steady flow. The component of wind velocity along the axis x is constant ($u_s=\text{const}$), and perpendicular component is equal zero ($v_s'=0$). These assumptions simplify calculation and estimate the critical reduced velocity. Hence the authors have carried out a series of calculations for different cylinder arrangements and different Scruton numbers. The obtained results can be presented in the form of a graph

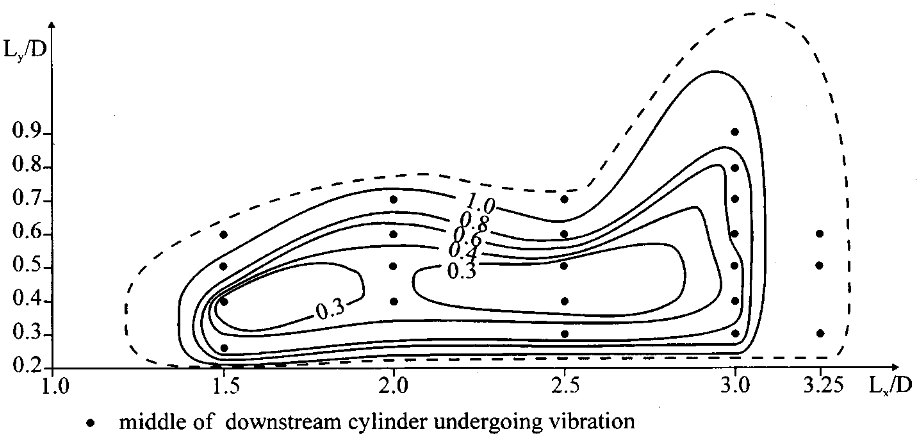

Fig. 4 Region of interference galloping with the line joining points of the same value of coefficient ψ (there is description in the text)

of the critical reduced velocity as function Sc. These graphs are nearly linear and they can be interpolated by straight line containing points $Sc=0$ and $U_r^{cr}=0$ with the slope of a straight line ψ $\left(\psi=\frac{U_r^{kr}}{Sc}\right)$. Finally all results of the calculation are shown in Fig. 4. There are lines joining points of the same value of coefficient ψ. The drop line is the boundary of the region of existing interference galloping for the steady flow.

Information from Fig. 4 could be used in engineering practice, if the wind had been the steady flow. Because it isn't, the influence of turbulence intensity on interference galloping should be checked.

5. Influence of turbulence intensity

In Fig. 3 it is seen that turbulence intensity induces rising of the critical reduced velocity. A difference between the value of the critical velocity for the steady flow and unsteady flow depends on the Scruton number.

Fig. 5 shows trajectories of cylinders at the steady and turbulence flows. In part a) of Figure the downstream cylinder moves along the regular ellipse. In parts b) and c) the flow turbulence causes that the movement of downstream cylinders has less regular form. In addition, the flow turbulence decreases extreme displacements. It should also be noticed that in all the cases the displacements of the upstream cylinder are considerably smaller than those of the downstream cylinder.

On the basis of Figs. 6 and 7 it can be said more about the significance of turbulence intensity. For example it is seen that the critical reduced velocity is a nonlinear rising function of turbulence intensity.

Fig. 6 presents directly the critical reduced velocity as a function of turbulence intensity. There are two plots for the location of the downstream cylinder outside the bistable flow region (comp. Ruscheweyh and Dielen 1992) and two plots for the location of the downstream cylinder inside it. For the former case vibrations of cylinders are forced by initial conditions for the steady and unsteady flows with small turbulence. The perturbations of flow induce cylinder movement for turbulence intensity bigger than about 10%. Value of the critical velocity is considerably greater in this case than in the second.

Fig. 7 shows the critical reduced velocity as a function of the Scruton number for different turbulence intensity. The graphs of the critical velocity go up and slopes of these straight lines decrease for greater turbulence intensity. It means that the bigger Scruton number is, the smaller influence of free stream turbulence on the critical reduced velocity is.

6. Conclusions

Basing upon presented results of numerical calculations the following conclusions can be formulated :

- Presented comparisons of experimental results and calculations confirm the correctness of the quasi-steady model of interference galloping (Fig. 3, Fig. 5) for wind tunnel models and elements, in which bending can be neglected such as ropes in a cable - stayed bridge.
- On the basis of calculation results obtained at steady flow, the reduced critical velocity

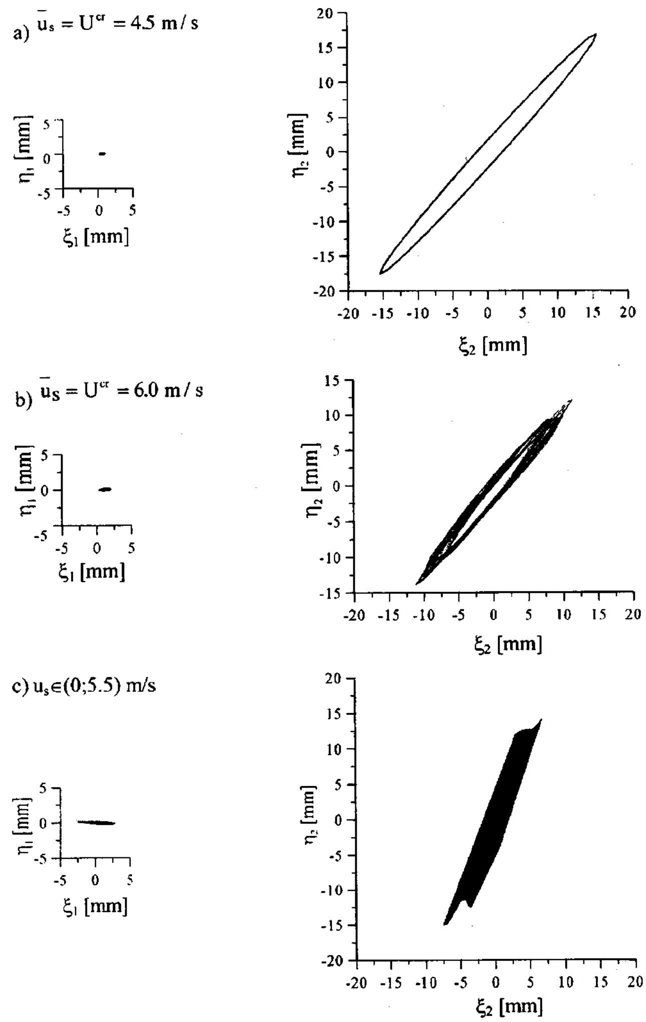

Fig. 5 Trajectory forms of cylinders; a) numerical results for steady flow; b) numerical for turbulence flow ($I_u = 12\%$); c) outline of measurement results in natural scale (on existing construction - cables of a cable-stayed bridge in Prague) presented by Studničkova (1994)

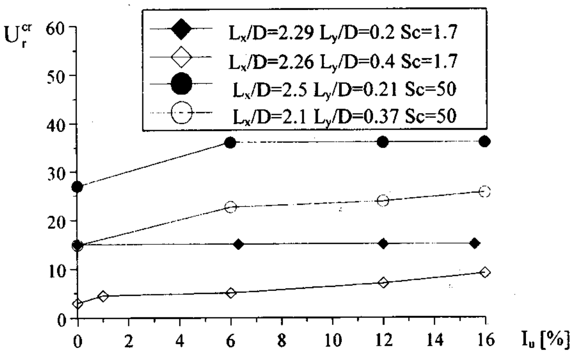

Fig. 6 Dependence of the reduced critical velocity U_r^{cr} on the turbulence intensity I_u and the distances between cylinders L_x/D and L_y/D

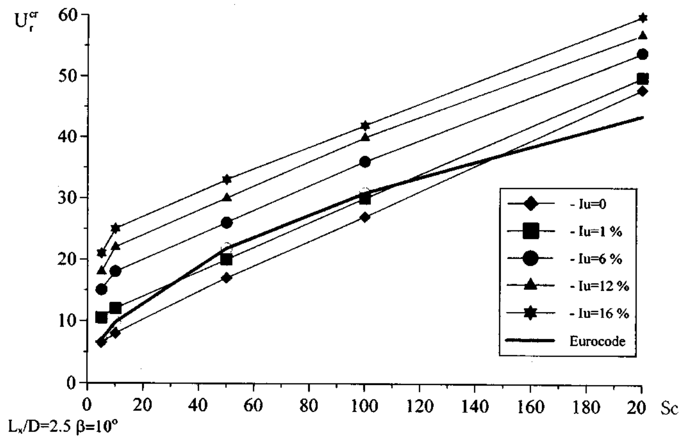

Fig. 7 Dependence of the reduced critical velocity U_r^{cr} on the turbulence intensity I_u and the Scruton number Sc for Lx/D=2.5 and Ly/D=0.44.

of wind can be evaluated and it can be used in engineering practice for Scruton number bigger than a border value. This border value of Scruton number depends on presumed evaluation accuracy of critical velocity.

- Fig. 7 shows comparison of numerical results and results, which are obtained on the basis of EUROCODE 1. It is seen that the latter values are values obtained for small turbulence intensity.
- Estimation of the critical velocity can be done with the help of Fig. 4 or Eq. (16).
- In future, the influence of heterogeneity of the analysed problem in the case of slender structures with circular cross section on the basic features of interference galloping ought to be checked.

References

Zdravkovich, M.M. and Pridden, D.L. (1977), "Interference between two identical circular cylinders; series of unexpected discontinuities", *J. of Ind. Aerodynamics*, **2**, 255-270.

Ruscheweyh, H (1983), "Aeroelastic interference effects between slender structures", *J. of Wind Eng. and Ind. Aerodynamics*, **14**, 129-140.

Ruscheweyh, H. and Dielen, B. (1992), "Interference galloping - investigations concerning the phase lag of the flow switching", *J. of Wind Eng. and Ind. Aerodynamics*, **41-44**, 2047-2056.

Kazakiewicz, M.I., Grafskij, I.J., Riedko, S.F. (1985), "Idientyfikacja ultragarmoniczeskich awtokolebanij pri aerodinamiczieskoj interfierencji tandema krugowych cilindrow w skoszennom potokie", Dokłady ukrainskoj akadiemi nauk, Kiev, 27-30.

Shiraishi, N., Matsumoto, M. and Shirato, H. (1986), "On aerodynamic instabilities of tandem structures", *J. of Wind Eng. and Ind. Aerodynamics*, **23**, 437-447.

Matsumoto, M., Shiraishi, N. and Shirato, H. (1990), "Aerodynamic instabilities of twin circular cylinders", *J. of Wind Eng. and Ind. Aerodynamics*, **33**, 91-100.

Sun, T.F. and Gu, Z.F. (1995), "Interference between wind loading on group of structures", *J. of Wind Eng. and Ind. Aerodynamics*, **54/55**, *The Proc. of 3rd Asia-Pacific Symp.* 1993, 1995, 213-225.

Błazik-Borowa, E., Flaga, A., Kazakiewicz, M.I. (1996), "Problems of interference galloping of two circular cylinders", *Studia z zakresu inżynierii*, **42**, Warsaw 1996.

Watzinger, J. (1996). Interferenzerregte Schwingungen zweier engstehender querangerströmter Zylinder, Dissertation TU Wien, 1996.

Sockel, H. and Watzinger, J. (1997), "Vibrations of two circular cylinders due to wind excited interference effects", *The Proc of 2nd European & African Conf. on Wind Eng.*, Genova, 1807-1813.

Dielen, B. and Ruscheweyh, H. (1995), "Mechanism of interference galloping of two identical circular cylinder in cross flow", *J. of Wind Eng. and Ind. Aerodynamics*, **54/55**, *The Proc. of 3rd Asia-Pacific Symp.* 1993, 1995, 289-300.

Błazik-Borowa, E. and Flaga, A. (1996), "Modelling of aerodynamic loads on a downstream cylinder caused by bistable flow between two circular cylinders", *J. of Wind Eng. and Ind. Aerodynamics*, **65**, 361-370.

Błazik-Borowa, E. and Flaga, A. (1995), "Quasi-steady models of aerodynamic loads on two circular cylinders in staggered arrangement", *The Proc. Ninth International Conference on Wind Engineering*, **1**, New Delhi, 95-107.

Zdravkovich, M. and Medeiros,E. (1991), "Effect of damping on interference-induced oscillations of two identical circular cylinders", *J. of Wind Eng. and Ind. Aerodynamic*, 197-211.

Studnička, M. (1994), "Induced vibrations of leeward ropes - A practical example", *The Proc. East European Conference on Wind Engineering "EECWE '94"*, Part 1, **3**, Warsaw, 49-59.

EUROCODE 1 : Part 6, Wind Loading. Draft, December 1993.

(Communicated by Giovanni Solari)